AGU100 ADVANCING EARTH AND SPACE SCIENCE

Earth and Space Science

TECHNICAL REPORTS: METHODS

10.1002/2017EA000318

Key Points:
- We created "Y-Mars," an analogue of a Martian mudstone explored by the Mars Science Laboratory
- We characterized the analogue material and highlight some of the inherent problems in producing analogues
- Our analogue has a number of applications for astrobiological research, but our process suggests more analogues are required

Supporting Information:
- Supporting Information S1

Correspondence to:
A. H. Stevens,
adam.stevens@ed.ac.uk

Citation:
Stevens, A. H., Steer, E., McDonald, A., Amador, E. S., & Cockell, C. S. (2018). Y-Mars: An astrobiological analogue of Martian mudstone. *Earth and Space Science*, *5*, 163–174. https://doi.org/10.1002/2017EA000318

Received 30 JUN 2017
Accepted 16 MAR 2018
Accepted article online 24 MAR 2018
Published online 19 APR 2018

Y-Mars: An Astrobiological Analogue of Martian Mudstone

Adam H. Stevens[1], Elizabeth Steer[2], Alison McDonald[3], Elena S. Amador[4], and Charles S. Cockell[1]

[1]UK Centre for Astrobiology, University of Edinburgh, Edinburgh, UK, [2]Nanoscale and Microscale Research Centre, The University of Nottingham, Nottingham, UK, [3]Bioimaging Facility, School of Engineering, University of Edinburgh, Edinburgh, UK, [4]California Institute of Technology, Pasadena, CA, USA

Abstract NASA's Mars Science Laboratory mission has collected evidence of a long-lasting habitable environment in the Sheepbed sediments of Gale Crater on Mars. The geochemistry of this mudstone suggests that the lake filling the crater in Mars' past had a neutral pH and low salinity and contained elements and redox couples required by life. We produced a geochemical analogue to the Sheepbed mudstone by mixing a collection of its primary minerals to match the X-Ray diffraction data from Mars Science Laboratory. Here we describe the production of the Y-Mars (Yellowknife-Mars) analogue and characterize its properties, including the presence of background carbon, nitrogen, and sulfur. We highlight some of the unavoidable issues involved in making analogues, especially for astrobiological applications. The Y-Mars analogue has a number of applications for astrobiological research, but more analogues are required to properly represent the diversity of Martian sedimentary contexts.

1. Introduction

Analogue research is used to advance our understanding and exploration of extraterrestrial surface and subsurface environments (Ehrenfreund et al., 2011, 2012; Payler et al., 2016; Preston & Dartnell, 2014). While terrestrial field analogue environments provide opportunities to study natural environments, laboratory analogues such as rock and soil simulants allow for more constrained testing and experimentation.

A number of Martian soil simulants have been developed over the years for a range of purposes. One of most widely used of these is JSC Mars-1/A, a weathered volcanic ash collected from Mauna Kea, Hawaii, which matches the reflectance spectrum of the widely distributed and unconsolidated dust/soil that covers much of the surface of Mars (bright regions) and also approximates the chemical composition, grain size, density, porosity, and magnetic parameters of Martian soil (Allen et al., 1998). However, while JSC Mars-1/A has been used in a number of research contexts (e.g., Chow et al., 2017; Court et al., 2014; Kral et al., 2004), it is primarily a spectral analogue, has limited applicability to the wide variety of environments on Mars that have been explored since its development, and is not well suited as an analogue for some terrestrial applications, for example, due to its hygroscopicity (Peters et al., 2008).

Analogue materials have been developed to aid in simulating the Martian surface, for example, for rover mobility studies (Brunskill et al., 2011; Zeng et al., 2015), geochemical simulations and instrument development (Peters et al., 2008; Scott et al., 2017), and aeolian simulations (Nørnberg et al., 2009). Other materials not specifically developed as analogues have also been used as Mars surface simulants in a wide variety of investigations (Jensen et al., 2014), including astrobiological research (Baqué et al., 2016; Böttger et al., 2012). However, little focus has been given to analogue materials that take into account recent in situ observations of mineralogy from previously habitable environments on Mars.

There is widespread evidence for sedimentary systems across the surface of Mars (e.g., Di Achille et al., 2006; Goudge et al., 2017; Squyres et al., 2004; Wray et al., 2008). Examples of these systems are high priorities for near-future exploration missions due to their favorable habitability and their ability to preserve any biomarkers that may have been emplaced in their sedimentary records (Hays et al., 2017). However, despite their widespread identification from orbit, detailed in situ measurements of these sedimentary systems are only available from the Mars Exploration Rover Opportunity and the Mars Science Laboratory (MSL).

The historical conditions of Gale Crater implied by analyses from MSL are significantly different from previously proposed aqueous Martian environments, including Meridiani Planum, which have generally been characterized as acidic (Bibring et al., 2005; Squyres et al., 2004). In contrast, the circumneutral, mildly

Table 1
Mineral Components of the Sheepbed Mudstone From the John Klein Drill Hole, as Identified by the CheMin Instrument

Mineral	Weight %
Plagioclase	22.4
Saponite smectite	22.0
Pigeonite	5.6
Augite	3.8
Magnetite	3.8
Orthopyroxene	3.0
Fe-forsterite	2.8
Anhydrite	2.6
Sanidine	1.2
Akageneite	1.1
Pyrrhotite	1.0
Bassanite	1.0
Amorphous	28.0

Note. Does not include <1% components. Taken from Vaniman et al. (2014).

saline waters of Gale Crater were long-lived, existing over millions to tens of millions of years of Mars' history (Grotzinger et al., 2014). All of the carbon, hydrogen, nitrogen, oxygen, phosphorus, and sulfur elements vital to terrestrial life have been detected in minerals or other compounds in the mudstones of Gale, as well as transition metals and plausible redox couples, although the bioavailability of these elements at the scale of microorganisms is unknown (McLennan et al., 2014; Ming et al., 2014; Stern et al., 2015; Vaniman et al., 2014). These data suggest that the lacustrine system at the base of Gale Crater, whose sediments eventually formed the Sheepbed mudstone, presents a record of a previously habitable Martian environment for which we have detailed in situ analyses.

We have constructed a laboratory simulant of the basic mineralogy of the Sheepbed sediments of Gale Crater, which we have used for astrobiological studies. Here we describe this analogue and some of its properties.

2. Materials and Methods

2.1. Analogue Composition

Material analogous to the Sheepbed mudstone was produced by combining minerals in the proportions detailed by CheMin measurements of the John Klein drill hole (Vaniman et al., 2014). The major minerals detected by CheMin are listed by weight percent in Table 1.

We removed the unidentified amorphous component and replaced components for which we could find no commercial sources. As noted by Vaniman et al. (2014), bassanite is rare on Earth due to quickly being hydrated when any moisture is present, so we replaced it with the selenite form of gypsum, which is widely available. Pigeonite and akaganeite, while not as rare on Earth, could not be procured commercially. Pigeonite was replaced with augite, which is closest in the pyroxene group solution series (Longhi & Bertka, 1996), though it contains a higher fraction of Ca. Akaganeite is generally found in hydrothermal systems and meteorites and is a weathering product of pyrrhotite (Ståhl et al., 2003). While the difference in chloride and sulfur compositions mean these minerals are not equivalent, pyrrhotite was the closest readily available replacement.

These combined ingredients (Table 2) were then used to assemble the analogue material. As the minerals were obtained from environmental sources, there were minor impurities, which were assessed by X-ray diffraction (XRD) analysis.

Table 2
Mineral Ingredients List for the Y-Mars Analogue Material

Mineral	Replacement sample	Weight %
Plagioclase	Albite	31.1
Saponite smectite	Saponite	30.5
Pigeonite	Augite	13.1
Augite	Augite	—
Magnetite	Magnetite	5.3
Orthopyroxene	Enstatite	4.2
Fe-forsterite	Dunite	3.9
Anhydrite	Anhydrite	3.6
Sanidine	Sanidine	1.7
Akaganeite	Pyrrhotite	2.9
Pyrrhotite	Pyrrhotite	—
Bassanite	Selenite	1.4

Mineral samples were obtained commercially (Richard Tayler Minerals, UK). They were ground separately by hand in a pestle and mortar to varying grain sizes, mixed by weight according to Table 2, and then ground further to a dry powder in an automated tungsten-carbide mill to form a "Y-Mars" (Yellowknife) analogue. The final grain size was measured using optical microscopy by dispersing a sample of the powder in ethanol onto a microscope slide and measuring 40 randomly selected grains on five fields of view at random locations on the slide.

2.2. XRD Analysis

The mineralogy of the analogue mixture was measured using a laboratory XRD (D8 Advance, Bruker, United States, with a Copper source at 1.54 Å) to confirm the expected mineral content and to allow for comparison of the diffractogram with the MSL CheMin instrument. The purity of the component minerals was assessed by scanning each component individually and performing Quantitative Rietveld

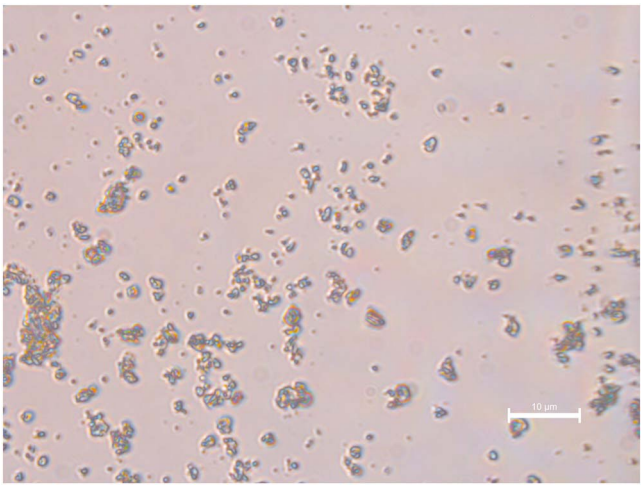

Figure 1. Optical micrograph of Y-Mars grains, with 10-μm scale bar.

analysis, using TOPAS software (Bruker, United States) to compare to known standards. When comparing directly to MSL data, the diffraction angle was scaled to match the CheMin instrument (Cobalt source at 1.79 Å).

2.3. XRF Analysis

Major element oxide concentrations were measured for the mixed analogue material and the saponite fraction with X-ray fluorescence (XRF) analysis (using a Panalytical PW2404 wavelength-dispersive sequential X-ray spectrometer). Glass discs of each sample were created by drying the sample overnight at 110°C, igniting a 1 g aliquot for 20 min at 1100°C in a Pt5%Au crucible, then reweighing to determine loss on ignition. The residue was mixed with Johnson Matthey Spectroflux 105 (lithium borate with a La_2O_3 heavy absorber) in a sample-to-flux ratio of 1:5 and fused for 20 min at 1100°C in a muffle furnace. Lost mass was made up by adding extra flux and fusing for a second time over a Meker burner then cast on a graphite mold on a 220°C hotplate and pressed with an aluminum plunger to create a flattened disk.

2.4. Visible/Shortwave Infrared Spectroscopy

The reflectance spectrum of the analogue material in the visible and shortwave infrared range between 350 and 2,500 nm was measured using an ASD FieldSpec Pro (ASD Inc., United States). The light source was at 0°, perpendicular to the sample plane, with the detector at 45°. Fifteen spectra were averaged and calibrated to absolute reflectance using a Spectralon calibration target. A comparator spectrum from Yellowknife Bay on Mars was collected from the Compact Reconnaissance Imaging Spectrometer for Mars (CRISM) instrument on the Mars Reconnaissance Orbiter (Murchie et al., 2007). Data were collected from CRISM image FRS00028346_01 by averaging a 3 × 3 pixel square from a location at sample 309, and line 72, approximated from Seelos et al. (2014). These orbital spectra were atmospherically corrected using the standard CRISM Analysis Tool v7.3.1 in ENVI and the standard bad channels were removed. Both the laboratory spectrum and the CRISM spectrum were normalized to their reflectance at 800 nm.

2.5. Raman Spectroscopy

Raman spectra were acquired with an inVia confocal Raman microscope (Renishaw, UK) with a Leica DMLM upright microscope, a 100X objective lens, and a 785-nm excitation laser. The instrument has a measured spot size of 1.2 (lateral) and 4 μm (axial) and a wavelength-dependent spectral resolution of between 6.5 and 7.6 cm^{-1}. Spectra were averaged over 3three different positions on each sample over the range 100–3,400 cm^{-1} with a 10 s exposure time and 70 mW excitation power. Spectra of minerals with high background fluorescence were acquired with lower laser power due to detector saturation. Spectra of magnetite and pyrrhotite were acquired with 8.5-mW excitation power, and saponite and the combined Y-Mars mixture were acquired with 34-mW excitation power. No sample damage was observed with the maximum laser power on all samples investigated. Wire 2.0 software was used for data acquisition and for cosmic ray removal from raw spectra.

2.6. Carbon, Nitrogen, and Sulfur Composition via Gas Chromatograph-Mass Spectrometery (GCMS)

Composition and isotope analysis for carbon, nitrogen, and sulfur was performed by Iso-Analytical Ltd., UK. In brief, C, N, and S isotope analysis of the acid-washed sediment samples was undertaken by elemental analyzer-isotope ratio mass spectrometry, using a Europa Scientific elemental analyzer. For C isotope analysis, samples were acidified with 1-M hydrochloric acid and left overnight to allow inorganic carbon to liberate as CO_2, then neutralized by washing with distilled water and oven dried at 60°C. The reference material used during ^{13}C and ^{15}N analysis was IA-R001 (wheat flour, $^{13}C_{V\text{-}PDB}$ = of −26.43‰, $^{15}N_{Air}$ = 2.55‰) and for ^{34}S analysis was IA-R061 (barium sulfate, $^{34}S_{V\text{-}CDT}$ = +20.33‰).

2.7. Pelleting

Samples of the Y-Mars analogue powder were pressed to form pellets of simulated mudstone. Given that Gale Crater is around 4.5 km deep (Grotzinger et al., 2014) and assuming a mudstone density of around

Table 3
Relative Purity of the Component Minerals in the Y-Mars Analogue and Additional "Contaminant" Minerals as Measured by Quantitative Rietveld analysis of XRD Data

Y-Mars Recipe Component	Intended weight %	Measured weight %
Albite	31.1	31.1
Saponite	30.5	n/a
Augite	13.1	15.1
Magnetite	5.3	1.3
Enstatite	4.2	3.3
Dunite	3.9	3.3
Anhydrite	3.6	3.4
Sanidine	1.7	1.7
Pyrrhotite	2.9	n/a
Selenite	1.4	1.4
Gypsum	0	0.1
Montmorillonite	0	0.1
Chlorite	0	1.2
Cordierite	0	2.3

Note. Minerals listed with n/a had no conclusive matches under Quantitative Rietveld analysis. XRD = X-ray diffraction.

2,200 kg/m^3 (Hobbs et al., 2002), the overburden pressure on the sediments forming the Sheepbed mudstone would have been around 35 MPa, assuming an upper limit of the crater being completely filled with sediment. Y-Mars pellets were created by pressing dried samples of the powder in a 13-mm diameter stainless steel press, cleaned with ethanol between each pellet. The 35-MPa pressure was supplied by a pneumatic vise.

3. Results

3.1. Analogue Material

The grain size of the Y-Mars powder has a range of 0.5–3.0 μm, with a mean of 1.2 μm and standard deviation of 0.5 μm. An example field of view is shown in Figure 1. This grain size is consistent with terrestrial definitions of a mudrock (< 32 μm) (Merriman et al., 2003) and with observations below the 60 μm resolution limit of the MAHLI instrument (Grotzinger et al., 2015) and therefore can be considered analogous to the fine-grained homogeneous mudstone observed using MAHLI in the Sheepbed unit.

3.2. XRD Analysis

The relative purity of the component minerals in the Y-Mars analogue is shown in Table 3. Full XRD traces are given in the supporting information.

The XRD diffractogram of the Y-Mars powder is shown in Figure 2, alongside the original data from the John Klein and Cumberland MSL drill holes from Vaniman et al. (2014). The major crystallographic peaks are all present in the analogue material, though there are minor angular shifts where the crystallographic peaks are not all directly coincident, most notably at the 2.53-Å magnetite peak at around 42° (Bristow et al., 2015). The peaks are well defined and narrow, but the relative intensity varies significantly and the lack of amorphous component in Y-Mars makes the crystallographic peaks more clearly separated. The smectite fraction of Y-Mars appears to match the Martian saponite according to the 02*l* band (Figure 2) and shows the 001

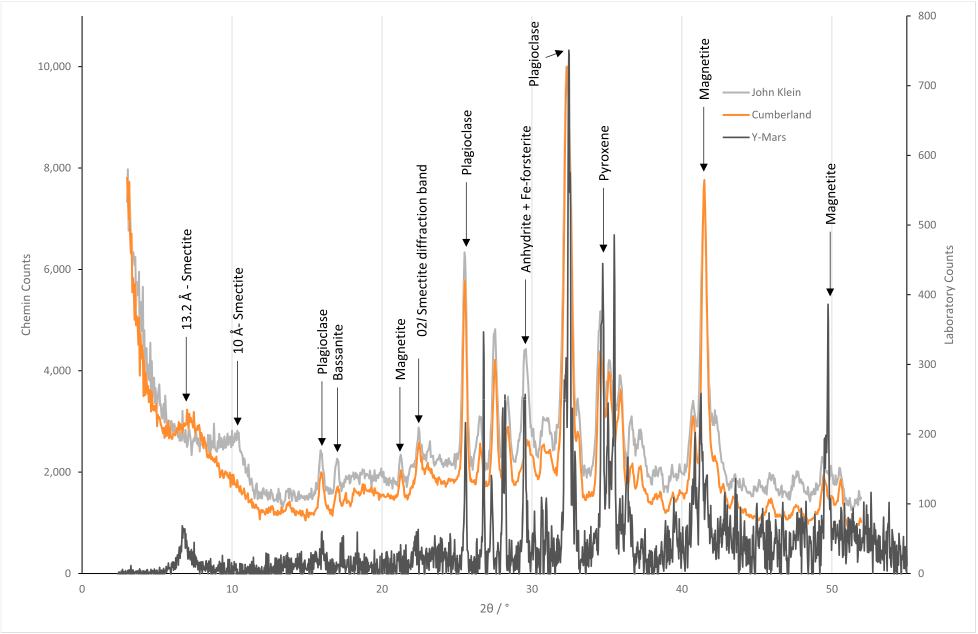

Figure 2. X-ray diffractograms of Y-Mars and two drill cores taken by Curiosity in the Yellowknife Bay mudstones. Labels following Vaniman et al. (2014), Treiman et al. (2014), and Bristow et al. (2015). Scattering angle of the Y-Mars diffractogram is scaled to match the Curiosity measurements.

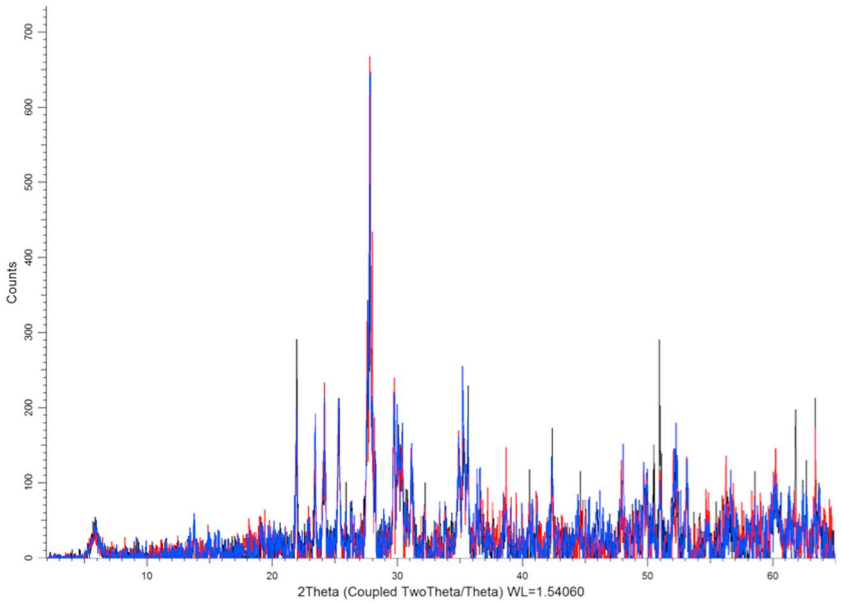

Figure 3. Three X-ray diffractograms (black, red, and blue) from different aliquots of the Y-Mars analogue material.

reflection at 13.2 Å but none at 10 Å, implying variation in interlayer cations and hydration state (Treiman et al., 2014).

Multiple X-ray diffractograms were measured to assess the heterogeneity of the Y-Mars material. These diffractograms are shown in Figure 3 and suggest some variability between different aliquots of Y-Mars, but quantitative Rietveld analysis suggests that this variation is less than 1% in compositional difference of the various minerals.

3.3. XRF Analysis

Major element compositions of the Y-Mars material and the saponite fraction are shown in Table 4. There was not enough available material of the other components of the analogue to allow XRF analysis.

3.4. Visible/Shortwave Infrared Spectroscopy

The reflectance spectrum of the Y-Mars analogue in the visible to near-infrared range is shown in Figure 4, alongside a spectrum of Yellowknife Bay obtained from orbit. The Y-Mars analogue material has an overall bluer reflectance than the Mars surface material observed from orbit, as expected for most Mars surface material which is typically covered in dust. The Y-Mars powder is broadly consistent with the Yellowknife Bay spectrum across the IR region, except at ~1.4 and 1.9 μm associated with OH/H_2O absorption features and ~2.15–2.3 μm likely associated with Al- and Fe/Mg-OH overtones. Y-mars is also similar to the spectral response of JSC Mars-1 and other simulants (Peters et al., 2008). Though the Yellowknife Bay surface mineralogy contains hydrated phases, these spectral signatures are difficult to detect from orbit, whereas they are evident in the Y-Mars due to the 1.9-μm hydration feature. The 3 × 3 pixel square used to collect the data represents an approximately 3.6 km^2 surface area reduced to a single spectrum, and our results are consistent with past studies looking for spectral signatures from orbit that are consistent with the MSL acquired mineralogy.

Table 4
Major Element Oxide Concentrations of the Y-Mars Analogue and Saponite Fraction

Oxide	Y-Mars (%)	Saponite Fraction (%)
SiO_2	44.97	48.12
Al_2O_3	13.31	12.38
Fe_2O_3	7.57	9.94
MgO	14.32	9.50
CaO	7.65	7.91
Na_2O	2.23	4.35
K_2O	0.08	0.39
TiO_2	0.77	0.47
MnO	0.18	0.11
P_2O_5	0.09	0.05
Loss on ignition	8.33	6.41

3.5. Raman Spectroscopy

Raman spectra of the individual mineral components and the mixed Y-Mars material are shown in Figures 5 and 6. All of the mineral components have diagnostic Raman peaks and some (augite, enstatite, and

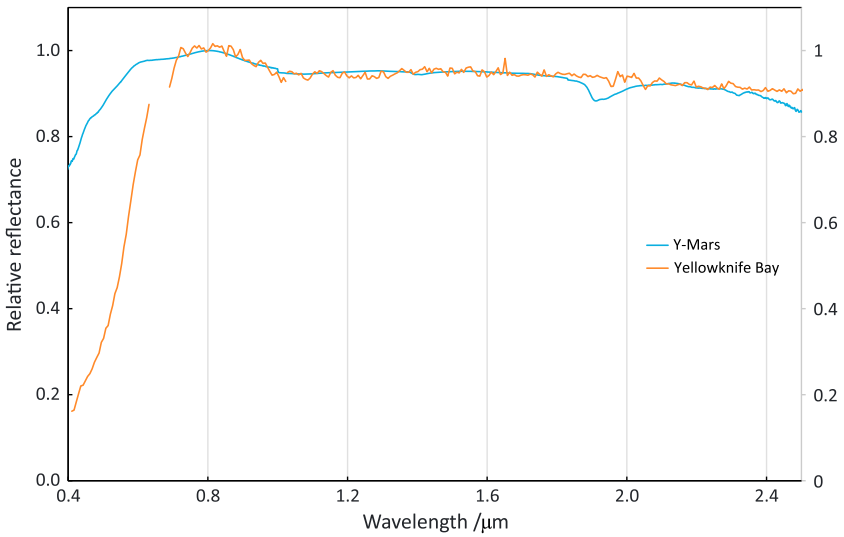

Figure 4. Reflectance spectrum of the Y-Mars analogue taken in the laboratory compared to an averaged Compact Reconnaissance Imaging Spectrometer for Mars spectra collected at Yellowknife Bay. Both spectra are ratioed to their reflectance at 800 nm. Gaps are due to bad channels in the Compact Reconnaissance Imaging Spectrometer for Mars instrument.

saponite) display a high degree of fluorescence. These diagnostic peaks generally match well with reference spectra for the minerals in the RRUFF database (Lafuente et al., 2015) or in the case of saponite, which is not listed in RRUFF, published literature (Wang et al., 1999).

The Raman spectrum of the combined mineral mixture has a high degree of heterogeneity at millimeter scales, as shown by the difference between the three spots (Figure 5). For example, there is a prominent peak at just over 1,000 cm^{-1}, which can be accounted for by the $\nu 1(SO_4)$ peak of the sulfate minerals (Berenblut et al., 1973) combined with the Si-O doublet from enstatite (Zucker & Shim, 2009). This peak is obvious in Spot 2, barely visible in Spot 1 and only apparent above the noise in Spot 3 by statistical extraction. There is also a peak at 500 cm^{-1}, perhaps from the plagioclase or sanidine, visible in Spots 2 and 3 but not in Spot 1. There is a high degree of fluorescence from the Y-Mars material, which is consistent with the response of the major saponite component.

3.6. Carbon, Nitrogen, and Sulfur Composition via GCMS

The total organic carbon and sulfur concentrations, as well as the carbon and sulfur fractionation measured in samples of Y-Mars and the individual mineral components, is shown in Table 5. There was insufficient nitrogen in any of the samples to measure above instrumental error of 10 ppm or allow for isotope analysis.

3.7. Pelleting

Pellets produced at 35 MPa had an appearance and texture similar to that of mudstone (Figure 7). A minimum amount of material was required to form a cohesive pellet, but thicknesses down to a few millimeters were possible.

4. Discussion

We produced an analogue of a Martian sedimentary rock using in situ mineralogical measurements of the Sheepbed mudstone collected by MSL. The analogue material, Y-Mars, is intended for use in relevant planetary science and astrobiological research and simulates what is thought to have been a habitable sedimentary environment on Mars (Grotzinger et al., 2014). Our results show that Y-Mars is comparable in mineralogy to the Sheepbed mudstone and in spectral reflectivity to general Mars surface material in the area of Yellowknife Bay.

The Sheepbed mudstone contains a number of minerals that are rare on Earth (Vaniman et al., 2014), but these are minor constituents and were replaced with comparable minerals that could be sourced

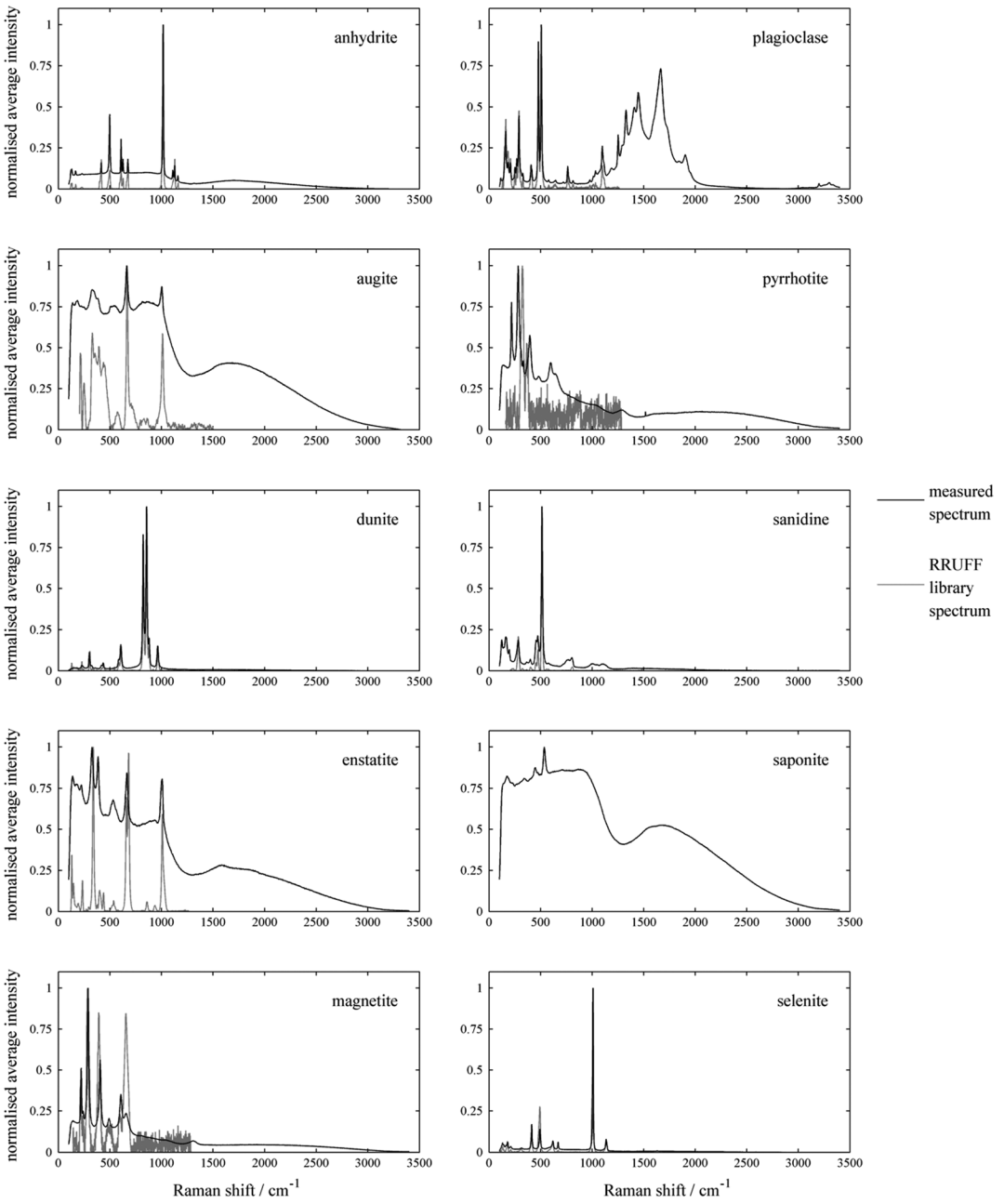

Figure 5. Raman spectra of the mineral components of the Y-Mars analogue, compared to library spectra from RRUFF. Each measured spectrum is averaged from three spots on a powdered mineral sample. Library spectra for saponite were not available.

commercially where possible. The major issue when producing the analogue was collecting enough saponite, which is a major constituent of the mudstone. Commercial sources of saponite were not abundant, and what we could acquire had to be carefully picked out of vesicles in basalt, which is where it is generally found (Cowking et al., 1983), a time-consuming process. Given that synthetic saponite is not straightforward to create in the laboratory and requires specialized equipment (Trujillano et al., 2011), this mineral proved to be the limiting factor in how much analogue we could produce. The other major component of the Sheepbed mudstone not included in Y-Mars was the amorphous minerals quantified but not compositionally constrained by CheMin XRD analysis. While this additional material could have a large impact on relevant properties of the analogue, such as the bioavailability of elements (Barber, 1995),

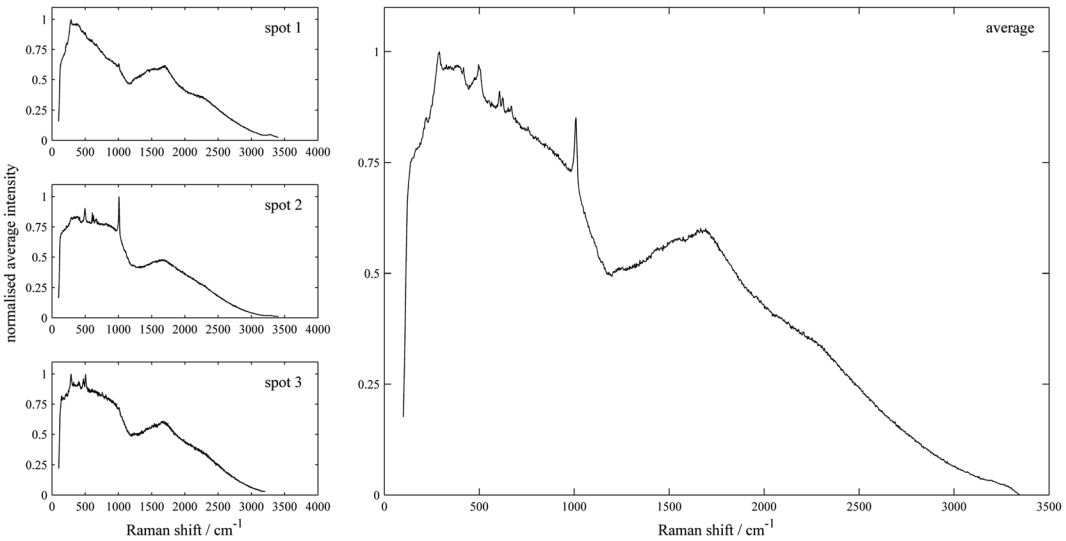

Figure 6. Raman spectra of the combined Y-Mars material. The three spots are shown on the left, with the average of these on the right.

especially soluble chloride and sulfur salts that would have a potentially large effect on the chemistry of the analogue in solution, including it would require correlating elemental abundances measured by the CheMin XRF instrument (McLennan et al., 2014) with minerals identified by XRD (Vaniman et al., 2014) to identify the elemental composition of the amorphous component (Morris et al., 2013), and then producing glassy material to match this elemental composition. This process was considered beyond the scope of this work.

The minerals (which were acquired essentially "blind") were measured by XRD to be high-purity samples, with the exception of the magnetite and enstatite, which had high levels of various associated silicate minerals. Given that the components with lower purity formed small fractions of the analogue material, the "contaminant minerals" (Table 3) are minor components of the final Y-Mars composition. Finding directly comparable minerals in terrestrial environments to use in analogues of Martian materials will naturally come with an associated level of impurity, especially given their rarity, but judicious collection and curation (for the community to use) would reduce this issue. Inclusion of the rarer and amorphous components or purer (perhaps synthetic) minerals could bring the crystallographic comparisons closer, but overall, the Y-Mars material is comparable to the Sheepbed mudstone to within a few percent composition. The lack of the amorphous component would have implications for the use of Y-Mars in experiments in solution, for example, using it as a substrate for microbial growth, but this could be counteracted by supplementing some of the missing elements. The clay fraction is also biologically important, especially given its high surface area, and so care should be taken to match this as closely as possible to the measured Martian clays in both mineralogical composition and interlayer spacing.

Table 5
Carbon and Sulfur Composition and Isotopic Fractionation of the Y-Mars Analogue and Component Minerals

Material	Wt%	Organic carbon (ppm)	$\delta^{13}C_{V\text{-}PDB}$ (‰)	Sulfur (%)	$\delta^{34}S_{V\text{-}CDT}$ (‰)
Y-Mars	100	1,110	−27.54	1.735	4.55
Albite	31.1	350	—	0.013	—
Saponite	30.5	1,040	−27.74	0.014	12.38
Augite	13.1	670	−26.59	0.045	10.75
Magnetite	5.3	490	−26.80	0.023	—
Enstatite	4.2	750	−26.96	0.035	—
Dunite	3.9	350	—	0.024	9.25
Anhydrite	3.6	90	—	23.228	12.36
Sanidine	1.7	370	—	0.053	1.93
Pyrrhotite	2.9	620	−27.67	24.377	2.12
Selenite	1.4	340	—	18.607	−17.03

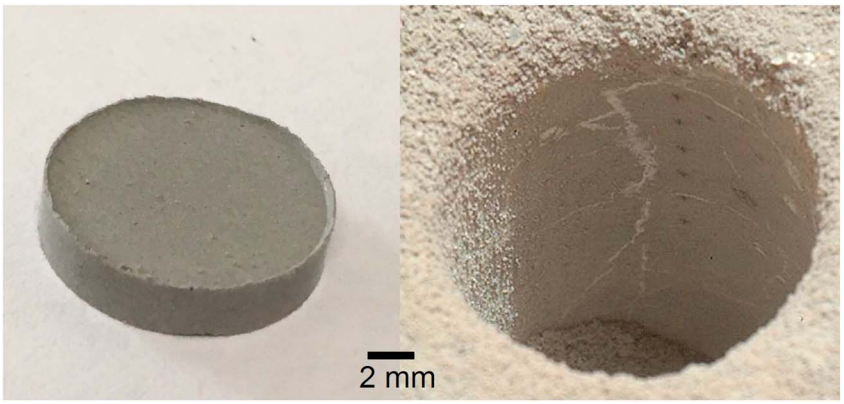

Figure 7. A Y-Mars pellet, 13 mm in diameter, compared to scale with the John Klein drill hole, which contained the material Y-Mars simulates. Note the sulfate-filled hairline fractures in the mudstone (Grotzinger et al., 2014).

While it is not possible in a laboratory setting to reproduce the millions of years of burial the Sheepbed mudstone may have experienced (Grotzinger et al., 2014), the pellets that can be produced in a press could be used to test instruments designed to investigate Martian sedimentary environments (Figure 7). Given that many of these instruments require ingestion of a sample, having an analogue with similar mechanical properties would be useful for testing. Other planned Mars instruments require sample processing and ingestion before analysis (Mahaffy et al., 2012; Parro et al., 2011). Having analogue material with similar mechanical properties would aid in the development of sample acquisition tools, though further in situ measurements of the mechanical properties would allow for more representative analogues to be produced, and other diagenetic processing would also have to be considered to make the analogue truly representative.

Astrobiological investigations of past habitable environments on Mars rely on using a set of different instruments, and being able to validate and test instrumentation on appropriate analogues increases the chance of scientific success in these missions. For example, both the NASA Mars 2020 Rover and the European Space Agency ExoMars Rover feature Raman instruments in their scientific payloads. The Raman spectra of Y-Mars show that its constituent minerals display a number of Raman peaks in the 1,000- to 1,600-cm range that could interfere with the identification of organic molecules contained within such a sediment (Ellery & Wynn-Williams, 2003; Foucher et al., 2015). Our spectra also show that at micron scales, sedimentary material like this has a high degree of spatial variability, though the extent to which this is a problem is dependent on the spot size of the Raman instrument. The spot size of our instrument (1–4 μm) is far lower than those of the planned ExoMars (50 μm) and Mars 2020 (<100 μm for SHERLOC and ~1 mm for SuperCam) instruments (Abbey et al., 2017; Rull et al., 2017; Wiens et al., 2016), which will therefore be less effected by micron-scale variability, but also not as able to identify small features, including sedimentary-scale grain variation. The ability to separate identifying peaks is also dependent on the spectral resolution of the instrument. While we were able to observe peaks potentially diagnostic of Y-Mars constituent minerals, at lower resolution these may not be apparent. However, the instrument used in this study has a similar spectral resolution to that of the ExoMars Raman instrument (6–8 cm^{-1}) and the Mars 2020 SuperCam (10 cm^{-1}) (Rull et al., 2017; Wiens et al., 2016), meaning that spatial sensitivity should be similar. The SHERLOC instrument has a lower spectral resolution (50 cm^{-1}) but aims specifically to identify organic molecules so is not a direct comparison (Abbey et al., 2017). Given that sedimentary environments are high priority in near-future astrobiological missions to Mars (Hays et al., 2017), testing analytical methods using analogues such as Y-Mars would allow for mitigation strategies to be developed prior to flight.

GCMS measurements of the Y-mars material show low levels of organic carbon and nitrogen, and sulfur isotope fractionation of similar levels to similar measurements of these molecules in the Sheepbed mudstone (Franz et al., 2017; Freissinet et al., 2015; Stern et al., 2015), even though these were not supplemented when producing the analogue and were therefore endogenous to the mineral samples. These data show that the introduction of C, N, and S into analogue materials made from commercial sources is likely during their preparation. The clay phase in Y-Mars was the main contributor to the total organic carbon in the analogue, and while it would be possible to bake out organics from the analogue material, this introduces the possibility of

mineral alteration. Our data underline the need to characterize these contaminants, particularly if the analogue is to be used in astrobiological studies or investigations on Martian organics. Nevertheless, we also note that these contaminants introduced during the preparation of the analogue could be serendipitously useful for studying the fate of background biologically relevant volatiles during material processing and testing by instruments designed for the detection of organics and biosignatures.

Although we do not know if Mars hosted life, the potentially habitable conditions in Gale Crater provide a location to test the hypothesis that they contained life. While the Sheepbed mudstone used to produce the ingredient list for the Y-Mars analogue will differ mineralogically from the original sediment that formed it, Y-Mars or similar analogues could be used to simulate the lacustrine environment of Gale Crater or other Martian sedimentary environments. Many such environments have been proposed as landing sites for future missions (e.g., Jezero Crater, Mawrth Vallis, and Oxia Planum), and therefore, analogues of sedimentary Martian environments are of greater astrobiological interest than the purely volcanic analogues that have generally been used to date.

5. Conclusions

The Y-Mars analogue was assembled using minerals identified in Gale Crater mudrocks by the CheMin instrument on the Curiosity rover. This analogue is fundamentally different from previous Mars analogue materials, as it was designed using in situ mineral observations to simulate a known Martian lacustrine sedimentary environment that may have been habitable in Mars' past. Y-Mars is a fine-grained powder that contains a number of basaltic weathering products including iron-rich smectites, which sets it apart from analogue materials such as JSC Mars-1/A. Some of the minerals identified in the Martian mudstones are relatively rare on Earth, making it difficult to produce a directly comparable analogue, but geochemical analysis shows that Y-Mars is similar to the Sheepbed mudstone and has a reflectance spectrum that is comparable to the Yellowknife unit of Gale Crater as observed from orbit, which is also generally similar to JSC Mars-1/A.

The Y-mars analogue could be used in a number of experimental contexts. It can be pressed under simulated Martian conditions to approximate a mudstone comparable to the formations observed by Curiosity or used in its powdered form. Such an analogue is useful for the development of instruments that might be interested in analysis of biomarkers in Martian sedimentary systems, or performing astrobiological simulations of putative ecosystems in these types of environments. Further measurements of mudstones in the stratigraphic column of Gale Crater have shown a highly diverse mineralogy just for this rock type in a single system (Rampe et al., 2017), and we know from orbital and ground-based measurements that there are a wide range of sedimentary systems across the surface of Mars. This implies a rich diversity of environments that might be targeted by future missions and suggests that one analogue material will never be enough. We would encourage the development of further soil analogues which can more accurately simulate the wide diversity of environments on Mars recorded by in situ measurements to date.

Acknowledgments
This research was supported by the UK Science and Technology Facilities Council (STFC) under grant ST/M001261/1. We would like to thank David Vaniman for helping us with CheMin XRD data, Richard Tayler for his assistance in mineral sample acquisition, and Nick Odling for assistance with laboratory preparation and analysis. Raw data are available via the University of Edinburgh DataShare Service (datashare.is.ed.ac.uk https://doi.org/10.7488/ds/2303).

References

Abbey, W. J., Bhartia, R., Beegle, L. W., DeFlores, L., Paez, V., Sijapati, K., et al. (2017). Deep UV Raman spectroscopy for planetary exploration: The search for in situ organics. *Icarus*, *290*, 201–214. https://doi.org/10.1016/j.icarus.2017.01.039

Allen, C. C., Jager, K. M., Morris, R. V., Lindstrom, D. J., Lindstrom, M. M., & Lockwood, J. P. (1998). JSC MARS-1: A Martian soil simulant space 98.

Baqué, M., Verseux, C., Böttger, U., Rabbow, E., de Vera, J.-P. P., & Billi, D. (2016). Preservation of biomarkers from cyanobacteria mixed with Marslike regolith under simulated Martian atmosphere and UV flux. *Origins of Life and Evolution of Biospheres*, *46*(2), 289–310. https://doi.org/10.1007/s11084-015-9467-9

Barber, S. A. (1995). *Soil nutrient bioavailability: A mechanistic approach*. New York: John Wiley.

Berenblut, B. J., Dawson, P., & Wilkinson, G. R. (1973). A comparison of the Raman spectra of anhydrite ($CaSO_4$) and gypsum ($CaSO_4)_2H_2O$. *Spectrochimica Acta Part A: Molecular Spectroscopy*, *29*(1), 29–36. https://doi.org/10.1016/0584-8539(73)80005-4

Bibring, J.-P., Langevin, Y., Gendrin, A., Gondet, B., Poulet, F., Berthé, M., et al. (2005). Mars surface diversity as revealed by the OMEGA/Mars Express observations. *Science*, *307*(5715), 1576–1581. https://doi.org/10.1126/science.1108806

Böttger, U., de Vera, J. P., Fritz, J., Weber, I., Hübers, H. W., & Schulze-Makuch, D. (2012). Optimizing the detection of carotene in cyanobacteria in a Martian regolith analogue with a Raman spectrometer for the ExoMars mission. *Planetary and Space Science*, *60*(1), 356–362. https://doi.org/10.1016/j.pss.2011.10.017

Bristow, T. F., Bish, D. L., Vaniman, D. T., Morris, R. V., Blake, D. F., Grotzinger, J. P., et al. (2015). The origin and implications of clay minerals from Yellowknife Bay, Gale crater, Mars. *American Mineralogist*, *100*(4), 824–836. https://doi.org/10.2138/am-2015-5077CCBYNCND

Brunskill, C., Patel, N., Gouache, T. P., Scott, G. P., Saaj, C. M., Matthews, M., & Cui, L. (2011). Characterisation of Martian soil simulants for the ExoMars rover testbed. *Journal of Terramechanics*, *48*(6), 419–438. https://doi.org/10.1016/j.jterra.2011.10.001

Chow, B. J., Chen, T., Zhong, Y., & Qiao, Y. (2017). Direct formation of structural components using a Martian soil simulant. *Scientific Reports*, *7*(1), 1151. https://doi.org/10.1038/s41598-017-01157-w

Court, R. W., Sims, M. R., Cullen, D. C., & Sephton, M. A. (2014). Searching for life on Mars: Degradation of surfactant solutions used in organic extraction experiments. *Astrobiology*, *14*(9), 733–752. https://doi.org/10.1089/ast.2013.1105

Cowking, A., Wilson, M. J., Tait, J. M., & Robertson, R. H. S. (1983). Structure and swelling of fibrous and granular saponitic clay from Orrock Quarry, Fife, Scotland. *Clay Minerals*, *18*(1), 49–64.

Di Achille, G., Marinangeli, L., Ori, G. G., Hauber, E., Gwinner, K., Reiss, D., & Neukum, G. (2006). Geological evolution of the Tyras Vallis paleolacustrine system, Mars. *Journal of Geophysical Research*, *111*, E04003. https://doi.org/10.1029/2005JE002561

Ehrenfreund, P., McKay, C., Rummel, J. D., Foing, B. H., Neal, C. R., Masson-Zwaan, T., et al. (2012). Toward a global space exploration program: A stepping stone approach. *Advances in Space Research*, *49*(1), 2–48. https://doi.org/10.1016/j.asr.2011.09.014

Ehrenfreund, P., Röling, W., Thiel, C., Quinn, R., Sephton, M., Stoker, C., et al. (2011). Astrobiology and habitability studies in preparation for future Mars missions: Trends from investigating minerals, organics and biota. *International Journal of Astrobiology*, *10*(3), 239–253. https://doi.org/10.1017/S1473550411000140

Ellery, A., & Wynn-Williams, D. (2003). Why Raman spectroscopy on Mars?—A case of the right tool for the right job. *Astrobiology*, *3*(3), 565–579. https://doi.org/10.1089/153110703322610654

Foucher, F., Ammar, M.-R., & Westall, F. (2015). Revealing the biotic origin of silicified Precambrian carbonaceous microstructures using Raman spectroscopic mapping: A potential method for the detection of microfossils on Mars. *Journal of Raman Spectroscopy*, *46*(10), 873–879. https://doi.org/10.1002/jrs.4687

Franz, H. B., McAdam, A. C., Ming, D. W., Freissinet, C., Mahaffy, P. R., Eldridge, D. L., et al. (2017). Large sulfur isotope fractionations in Martian sediments at Gale crater. *Nature Geoscience*, *10*, 658. https://doi.org/10.1038/ngeo3002

Freissinet, C., Glavin, D. P., Mahaffy, P. R., Miller, K. E., Eigenbrode, J. L., Summons, R. E., et al. (2015). Organic molecules in the Sheepbed Mudstone, Gale Crater, Mars. *Journal of Geophysical Research: Planets*, *120*, 495–514. https://doi.org/10.1002/2014JE004737

Goudge, T. A., Milliken, R. E., Head, J. W., Mustard, J. F., & Fassett, C. I. (2017). Sedimentological evidence for a deltaic origin of the western fan deposit in Jezero crater, Mars and implications for future exploration. *Earth and Planetary Science Letters*, *458*, 357–365. https://doi.org/10.1016/j.epsl.2016.10.056

Grotzinger, J. P., Gupta, S., Malin, M., Rubin, D., Schieber, J., Siebach, K., et al. (2015). Deposition, exhumation, and paleoclimate of an ancient lake deposit, Gale crater, Mars. *Science*, *350*(6257), aac7575.

Grotzinger, J. P., Sumner, D. Y., Kah, L. C., Stack, K., Gupta, S., Edgar, L., et al. (2014). A habitable fluvio-lacustrine environment at Yellowknife Bay, Gale Crater, Mars. *Science*, *343*(6169). https://doi.org/10.1126/science.1242777

Hays, L. E., Graham, H. V., Des Marais, D. J., Hausrath, E. M., Horgan, B., McCollom, T. M., et al. (2017). Biosignature preservation and detection in Mars analog environments. *Astrobiology*, *17*(4), 363–400. https://doi.org/10.1089/ast.2016.1627

Hobbs, P. R. N., Hallam, J. R., Forster, A., Entwisle, D. C., Jones, L. D., Cripps, A. C., et al. (2002). Engineering geology of British rocks and soils—Mudstones of the Mercia Mudstone Group British Geological Survey Research Report (pp. 106).

Jensen, S. J. K., Skibsted, J., Jakobsen, H. J., ten Kate, I. L., Gunnlaugsson, H. P., Merrison, J. P., et al. (2014). A sink for methane on Mars? The answer is blowing in the wind. *Icarus*, *236*, 24–27. https://doi.org/10.1016/j.icarus.2014.03.036

Kral, T., Bekkum, C., & McKay, C. (2004). Growth of methanogens on a Mars soil simulant. *Origins of Life and Evolution of Biospheres*, *34*(6), 615–626. https://doi.org/10.1023/B:ORIG.0000043129.68196.5f

Lafuente, B., Downs, R. T., Yang, H., & Stone, N. (2015). *The power of databases: The RRUFF project*. Berlin: W. De Gruyter.

Longhi, J., & Bertka, C. M. (1996). Graphical analysis of pigeonite-augite liquidus equilibria. *American Mineralogist*, *81*, 685.

Mahaffy, P., Webster, C., Cabane, M., Conrad, P., Coll, P., Atreya, S., et al. (2012). The sample analysis at Mars investigation and instrument suite. *Space Science Reviews*, *170*(1–4), 401–478. https://doi.org/10.1007/s11214-012-9879-z

McLennan, S. M., Anderson, R. B., Bell, J. F., Bridges, J. C., Calef, F., Campbell, J. L., et al. (2014). Elemental geochemistry of sedimentary rocks at Yellowknife Bay, Gale Crater, Mars. *Science*, *343*(6169). https://doi.org/10.1126/science.1244734

Merriman, R. J., Highley, D. E., & Cameron, D. G. (2003). Definition and characteristics of very-fine grained sedimentary rocks: Clay, mudstone, shale and slate: British Geological Survey Commissioned Report.

Ming, D. W., Archer, P. D., Glavin, D. P., Eigenbrode, J. L., Franz, H. B., Sutter, B., et al. (2014). Volatile and organic compositions of sedimentary rocks in Yellowknife Bay, Gale Crater, Mars. *Science*, *343*(6169). https://doi.org/10.1126/science.1245267

Morris, R. V., Ming, D. W., Blake, D. F., Vaniman, D. T., Bish, D. L., Chipera, S. J., et al. (2013). *The amorphous component in Martian basaltic soil in global perspective from MSL and MER missions*. Paper presented at the Lunar and Planetary Science Conference. Retrieved from http://adsabs.harvard.edu/abs/2013LPI.44.1653M

Murchie, S., Arvidson, R., Bedini, P., Beisser, K., Bibring, J. P., Bishop, J., et al. (2007). Compact Reconnaissance Imaging Spectrometer for Mars (CRISM) on Mars Reconnaissance Orbiter (MRO). *Journal of Geophysical Research*, *112*, EO5S03. https://doi.org/10.1029/2006JE002682

Nørnberg, P., Gunnlaugsson, H. P., Merrison, J. P., & Vendelboe, A. L. (2009). Salten Skov I: A Martian magnetic dust analogue. *Planetary and Space Science*, *57*(5–6), 628–631. https://doi.org/10.1016/j.pss.2008.08.017

Parro, V., de Diego-Castilla, G., Rodríguez-Manfredi, J. A., Rivas, L. A., Blanco-López, Y., Sebastián, E., et al. (2011). SOLID3: A multiplex antibody microarray-based optical sensor instrument for in situ life detection in planetary exploration. *Astrobiology*, *11*(1), 15–28. https://doi.org/10.1089/ast.2010.0501

Payler, S. J., Biddle, J. F., Coates, A. J., Cousins, C. R., Cross, R. E., Cullen, D. C., et al. (2016). Planetary science and exploration in the deep subsurface: Results from the MINAR Program, Boulby Mine, UK. *International Journal of Astrobiology*, *16*(2), 114–129. https://doi.org/10.1017/S1473550416000045

Peters, G. H., Abbey, W., Bearman, G. H., Mungas, G. S., Smith, J. A., Anderson, R. C., et al. (2008). Mojave Mars simulant—Characterization of a new geologic Mars analog. *Icarus*, *197*(2), 470–479. https://doi.org/10.1016/j.icarus.2008.05.004

Preston, L. J., & Dartnell, L. R. (2014). Planetary habitability: Lessons learned from terrestrial analogues. *International Journal of Astrobiology*, *13*(01), 81–98. https://doi.org/10.1017/S1473550413000396

Rampe, E. B., Ming, D. W., Blake, D. F., Bristow, T. F., Chipera, S. J., Grotzinger, J. P., et al. (2017). Mineralogy of an ancient lacustrine mudstone succession from the Murray formation, Gale crater, Mars. *Earth and Planetary Science Letters*, *471*, 172–185. https://doi.org/10.1016/j.epsl.2017.04.021

Rull, F., Maurice, S., Hutchinson, I., Moral, A., Perez, C., Diaz, C., et al. (2017). The Raman laser spectrometer for the ExoMars Rover mission to Mars. *Astrobiology*, *17*(6–7), 627–654. https://doi.org/10.1089/ast.2016.1567

Scott, A. N., Oze, C., Tang, Y., & O'Loughlin, A. (2017). Development of a Martian regolith simulant for in-situ resource utilization testing. *Acta Astronautica*, *131*, 45–49. https://doi.org/10.1016/j.actaastro.2016.11.024

Seelos, K. D., Seelos, F. P., Viviano-Beck, C. E., Murchie, S. L., Arvidson, R. E., Ehlmann, B. L., & Fraeman, A. A. (2014). Mineralogy of the MSL Curiosity landing site in Gale crater as observed by MRO/CRISM. *Geophysical Research Letters*, *41*, 4880–4887. https://doi.org/10.1002/2014GL060310

Squyres, S. W., Grotzinger, J. P., Arvidson, R. E., Bell, J. F., Calvin, W., Christensen, P. R., & Soderblom, L. A. (2004). In situ evidence for an ancient aqueous environment at Meridiani Planum, Mars. *Science*, *306*(5702), 1709–1714. https://doi.org/10.1126/science.1104559

Ståhl, K., Nielsen, K., Jiang, J., Lebech, B., Hanson, J. C., Norby, P., & van Lanschot, J. (2003). On the akaganéite crystal structure, phase transformations and possible role in post-excavational corrosion of iron artifacts. *Corrosion Science*, *45*(11), 2563–2575. https://doi.org/10.1016/S0010-938X(03)00078-7

Stern, J. C., Sutter, B., Freissinet, C., Navarro-González, R., McKay, C. P., Archer, P. D., et al. (2015). Evidence for indigenous nitrogen in sedimentary and aeolian deposits from the Curiosity rover investigations at Gale crater, Mars. *Proceedings of the National Academy of Sciences*, *112*(14), 4245–4250. https://doi.org/10.1073/pnas.1420932112

Treiman, A. H., Morris, R. V., Agresti, D. G., Graff, T. G., Achilles, C. N., Rampe, E. B., & Downs, R. T. (2014). Ferrian saponite from the Santa Monica Mountains (California, U.S.A., Earth): Characterization as an analog for clay minerals on Mars with application to Yellowknife Bay in Gale Crater. *American Mineralogist*, *99*(11–12), 2234–2250. https://doi.org/10.2138/am-2014-4763

Trujillano, R., Rico, E., Vicente, M. A., Rives, V., Ciuffi, K. J., Cestari, A., & Korili, S. A. (2011). Rapid microwave-assisted synthesis of saponites and their use as oxidation catalysts. *Applied Clay Science*, *53*(2), 326–330. https://doi.org/10.1016/j.clay.2010.12.005

Vaniman, D. T., Bish, D. L., Ming, D. W., Bristow, T. F., Morris, R. V., Blake, D. F., & Team, M. S. (2014). Mineralogy of a mudstone at Yellowknife Bay, Gale Crater, Mars. *Science*, *343*(6169). https://doi.org/10.1126/science.1243480

Wang, A., Jolliff, B. L., & Haskin, L. A. (1999). Raman spectroscopic characterization of a highly weathered basalt: Igneous mineralogy, alteration products, and a microorganism. *Journal of Geophysical Research*, *104*(E11), 27,067–27,077. https://doi.org/10.1029/1999JE001071

Wiens, R. C., Maurice, S., Mccabe, K., Cais, P., Anderson, R. B., Beyssac, O., & Dromart, G. (2016). *The SuperCam remote sensing instrument suite for Mars 2020*. Paper presented at the 47th Lunar and Planetary Science Conference.

Wray, J. J., Ehlmann, B. L., Squyres, S. W., Mustard, J. F., & Kirk, R. L. (2008). Compositional stratigraphy of clay-bearing layered deposits at Mawrth Vallis, Mars. *Geophysical Research Letters*, *35*, L12202. https://doi.org/10.1029/2008GL034385

Zeng, X., Li, X., Wang, S., Li, S., Spring, N., Tang, H., & Feng, J. (2015). JMSS-1: A new Martian soil simulant. *Earth, Planets and Space*, *67*(1), 72. https://doi.org/10.1186/s40623-015-0248-5

Zucker, R., & Shim, S.-H. (2009). In situ Raman spectroscopy of MgSiO3 enstatite up to 1550 K. *American Mineralogist*, *94*(11–12), 1638–1646. https://doi.org/10.2138/am.2009.3210